ACS Biomaterials SCIENCE & ENGINEERING

pubs.acs.org/journal/abseba

Article

Electrochemical Biosensor Based on HRP/Ti_3C_2/Nafion Film for Determination of Hydrogen Peroxide in Serum Samples of Patients with Acute Myocardial Infarction

Wei Xu, Marwan Sakran, Jianwen Fei, Xiaoyun Li, Chenyuan Weng, Wei Yang, Guomin Zhu, Wanying Zhu,* and Xuemin Zhou*

Cite This: *ACS Biomater. Sci. Eng.* 2021, 7, 2767−2773

Read Online

ACCESS | Metrics & More | Article Recommendations | Supporting Information

ABSTRACT: Hydrogen peroxide (H_2O_2) has been reported to mediate a variety of physiological and pathological processes in living systems. In this work, a biosensor for determination of H_2O_2 was prepared by using an HRP/Ti_3C_2/Nafion film-modified glassy carbon electrode (GCE). Ti_3C_2 nanosheets with remarkable conductivity and high specific surface area were chosen as carriers for HRP. Moreover, this biosensor modified with HRP has a specific catalytic effect on H_2O_2. The difference in peak current could reflect the quantitative change of H_2O_2. The linear range of the biosensor is 5−8000 μM, and the detection limit is 1 μM ($S/N = 3$). This biosensor was used to detect H_2O_2 in clinical serum samples of normal controls and patients with acute myocardial infarction (AMI) before and after percutaneous coronary intervention (PCI). The results showed that the difference between normal controls and patients is significant ($P < 0.05$), as well as the difference for patients before and after PCI ($P < 0.01$), but no significant difference existed between postoperative patients and normal controls. This biosensor has the advantages of simple preparation, high sensitivity, and quick detection, showing potential application in clinical diagnosis.

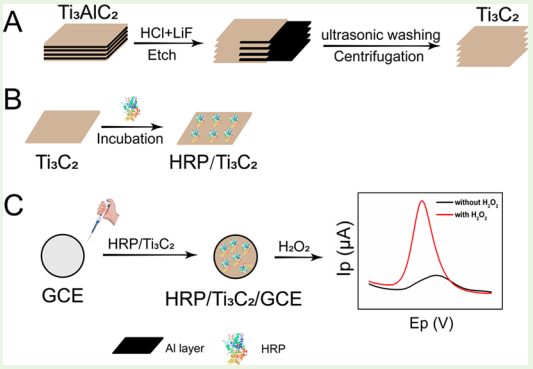

KEYWORDS: *MXene, Ti_3C_2, electrochemical biosensor, hydrogen peroxide, acute myocardial infarction*

1. INTRODUCTION

In living systems, H_2O_2 is produced by aerobic respiration, acts as a messenger for various signal transduction pathways, and also serves as an important indicator for molecular diagnosis.[1] The accumulation of overgenerated H_2O_2 in oxidative stress status is presented in many cardiovascular diseases, such as acute myocardial infarction (AMI).[2] AMI is an event of myocyte necrosis caused by rupture or erosion of unstable coronary atherosclerotic plaque. As a common cardiac emergency, it has the potential for substantial morbidity and mortality worldwide.[3] Percutaneous coronary intervention (PCI) is the evidence-based standard and an effective treatment for AMI patients.[4] This reperfusion therapy significantly relieves angina symptoms and reduces mortality in such patients.[5−7] There is an imbalance between oxidants and antioxidants in AMI, which is manifested by the reduction of such species as superoxide dismutase (SOD) and catalase (CAT). This alteration resulted in a reduced antioxidant ability on decomposing superoxide anion and H_2O_2, leading to oxidative damage in the myocyte.[8] PCI effectively reduced biochemically assessed oxidative stress and myocardial damage. AMI often began quickly and was characterized by a sudden burst of crushing heart pain and a feeling of near-death. H_2O_2 may be an important indicator of AMI. Thus, the measurement of H_2O_2 levels is of great significance for an in-depth understanding of the pathogenesis underlying AMI and clinical effects of reperfusion therapy by PCI.

Electrochemical sensors use electrodes as signal converters to measure electric potential or current. It usually consists of two parts: molecular recognition and information conversion.[9] Biosensors, especially electrochemical enzyme biosensors, have excellent selectivity, high sensitivity, and easy operation, which can realize in situ real-time detection.[10] However, the biological enzyme, which has poor stability and a short life, is usually sensitive to temperature and pH. Therefore, the signal from the enzyme sensor is easily disturbed by the external environment and affected by the change of analysis conditions.[11−13] Hence, we should try to find a simple and reliable immobilized enzyme scheme to overcome these

Received: February 18, 2021
Accepted: April 26, 2021
Published: May 4, 2021

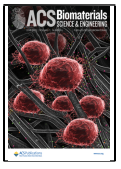

https://doi.org/10.1021/acsbiomaterials.1c00242
ACS Biomater. Sci. Eng. 2021, 7, 2767−2773

shortcomings.[14−16] The development of new immobilized platforms to improve the stability of enzymes to the environment is an important research topic to realize the commercialization of enzyme sensors.[17−20]

As a new type of 2D nanomaterial, MXene has received extensive attention because of its advantages such as superior conductivity, good hydrophilicity, a large surface, and easy film formation.[21,22] The general formula of MXene is $M_{n+1}X_nT_x$, where M represents the transition metal, X represents C or N, n could be between 1 and 3, and T_x represents different functional groups on the surface of MXene.[23] MXene is considered to be an appreciable nanomaterial because of its distinct layered structure and good biocompatibility.[24,25] Compared with other types of 2D nanomaterials, MXene has the benefits of predominant surface electrochemical activity, high metal conductivity, and good dispersion in aqueous solution. Ti_3C_2 is the most typical representative of MXene; it has attracted extensive attention from electrochemical researchers due to its excellent electrochemical response, catalytic performance, and electron conduction ability.[26] Thereby, MXene could serve as an excellent immobilization platform. The combination of MXene with the biological enzyme can improve the stability of the biological enzyme and the sensitivity of the determination, which is a good strategy to solve the shortcomings of biological enzyme sensors.

In this work, a novel electrochemical biosensor based on HRP/Ti_3C_2/Nafion film was prepared for the determination of H_2O_2. Compared to numerous hydrogen peroxide sensors reported in recent years,[27,28] the advantages of HRP/Ti_3C_2/Nafion-modified electrochemical biosensor include the following points. First, the high conductivity of Ti_3C_2 nanosheets can promote the electron transfer at the electrode surface and amplify the H_2O_2 signal, improving the sensitivity of the electrochemical biosensor. Second, the biosensor modified with HRP has a specific catalytic effect on H_2O_2. Moreover, the HRP/Ti_3C_2/Nafion-modified electrochemical biosensor has good stability. Last, the biosensor is easy to operate and can realize in situ real-time detection, which has high clinical application value. The electrochemical biosensor provided an important reference index for clinical workers in real-time diagnosis of AMI and evaluation of a therapy effect. In addition, the designed HRP/Ti_3C_2/Nafion biosensor showed good sensitivity and selectivity to H_2O_2, and it was therefore first used for H_2O_2 detection of serum samples from AMI patients. The changes in H_2O_2 levels of patients before and after PCI were analyzed and compared. This work has an important application prospect in real-time diagnosis of acute myocardial infarction disease and evaluation of a surgical treatment effect.

2. EXPERIMENTAL PROCESS

2.1. Reagents and Materials. Horseradish peroxidase (HRP) was purchased from Aladdin Reagent (Shanghai, China). Hydrogen peroxide (H_2O_2, 30%) was purchased from Shanghai Lingfeng Chemical Reagent Co., Ltd. (Shanghai, China). Ti_3AlC_2 MAX was purchased from Jilin 11 Technology Co. Lysozyme (Lys) (Jilin, China). Lithium fluoride (LiF), hydrochloric acid (HCl), ascorbic acid (AA), uric acid (UA), glucose (Glu), citric acid (CA), and urea were obtained from Sinopharm Chemical Reagent Co., Ltd. (Shanghai, China). Nafion (5%) was purchased from Sigma−Aldrich. The ultrapure water used in all processes comes from the Millipore water purification system.

2.2. Apparatus. The electrochemical measurement was performed on a traditional three-electrode battery using a CHI 660D workstation (Shanghai Chenhua Co., China). The platinum electrode is the counter electrode, and the saturated calomel electrode (SCE) is the reference electrode. GCE (glassy carbon electrode, D = 5 mm) was purchased from Tianjin Incole Union Technology Co., Ltd. (Tianjin, China). The JEM-2100 instrument (JEOL, Japan) was used for the transmission electron microscope (TEM) and high resolution transmission electron microscope (HRTEM) images. The phase structure of the samples was characterized by a Rigaku Smartlab X-ray diffractometer.

2.3. Synthesis of Ti_3C_2. Ti_3C_2 was prepared using the previously reported method.[29] As shown in part A of Scheme 1, 1 g of LiF was dissolved completely in 20 mL of 6 M HCl, and this was stirred at room temperature to obtain a LiF/HCl solution. Then, 1 g of Ti_3AlC_2 was slowly added to the LiF/HCl solution. The temperature of the suspension was increased to 35 °C, and stirring continued for 24 h. The reaction solution was repeatedly washed with ultrapure water and centrifuged at 1100g until the supernatant was neutral. After that, the suspension was centrifuged at 6000g to take Ti_3C_2 in the supernatant for later use.

Scheme 1. Construction of HRP/Ti_3C_2 Biosensor and the Determination of H_2O_2

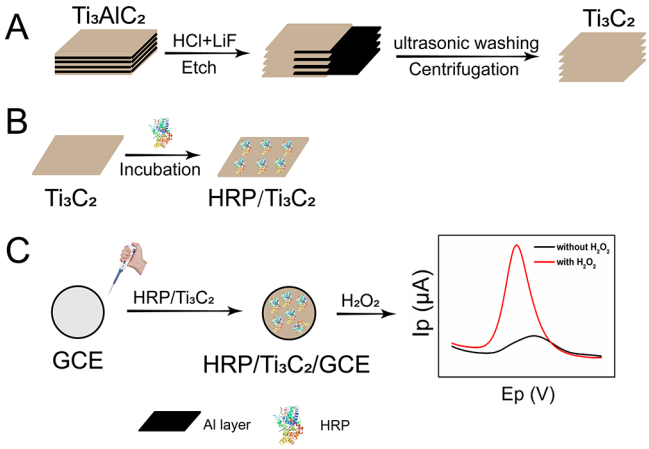

2.4. Fabrication of the HRP/Ti_3C_2/Nafion/GCE Biosensor. The GCE was first polished using Al_2O_3 powder and then washed with ultrasonic water three times. As shown in part B of Scheme 1, 6 μL of HRP solution (10 mg mL^{-1}) was mixed with 16 μL of Ti_3C_2 solution (1.25 mg mL^{-1}), followed by 16.6 μL of PBS (5 mM, pH 7.4). Finally, 1.4 μL of Nafion was mixed and shaken at 37 °C 800 rpm for 30 min. A 15 μL portion of the resultant HRP/Ti_3C_2/Nafion mixture was dropped to the previously prepared standby GCE surface. The prepared electrodes (HRP/Ti_3C_2/Nafion/GCE) were dried and stored at 4 °C prior to usage.

2.5. Determination of H_2O_2. As shown in part C of Scheme 1, for the H_2O_2 electrochemical determination, we added different concentrations of H_2O_2 to a mixed solution of 200 μL of KCl (1 M) and 200 μL of PBS (0.5 mM) and diluteded this to 2 mL. Next, HRP/Ti_3C_2/Nafion/GCE was slowly inserted into the mixed solution. Then, a differential pulse voltammetry (DPV) measurement was performed in the scan range −0.8 to 0.2 V at a scan rate of 100 mV s^{-1}, and the pulse width, pulse period, and quiet time were 0.025, 0.1, and 2 s, respectively.

2.6. Analysis of H_2O_2 from Serum. We explored the application of this method to the determination of H_2O_2 in human serum from normal controls and AMI patients (preoperation and postoperation of PCI). First, 100 μL serum samples were mixed with 300 μL of methanol and centrifuged at 15 000g for 5 min. Then, 200 μL of the supernatant was taken to perform the determination according to the method described in "Determination of H_2O_2". The results were statistically analyzed by an independent t test or paired t test. A P value less than 0.05 indicates that the sample data are significantly different.

https://doi.org/10.1021/acsbiomaterials.1c00242
ACS Biomater. Sci. Eng. 2021, 7, 2767−2773

3. RESULTS AND DISCUSSION

3.1. Characterization of Ti_3C_2. TEM characterization indicated the typical 2D exfoliation morphology of Ti_3C_2 after LiF + HCl etching. As shown in the TEM image (Figure 1A),

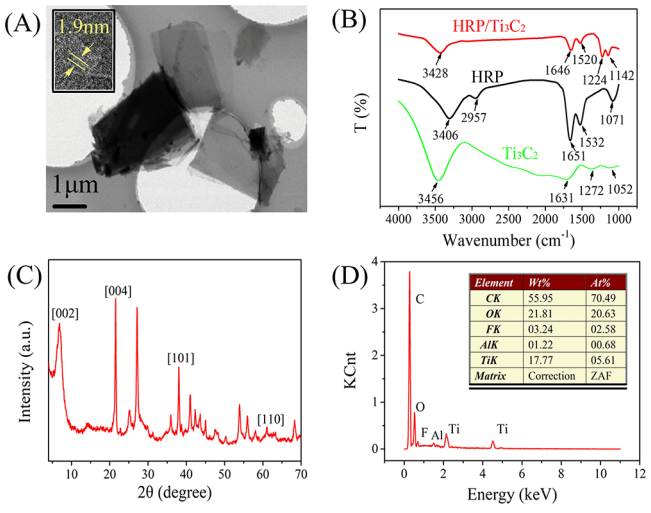

Figure 1. (A) TEM image of the Ti_3C_2. Inset: HRTEM image. (B) FT-IR of the biosensor. (C) XRD pattern of Ti_3C_2. (D) EDS spectrum of the Ti_3C_2.

the Ti_3C_2 nanosheets showed an obvious two-dimensional lamellar structure. In addition, the HRTEM image further reveals the crystal characteristics of Ti_3C_2. The adjacent lattice fringe with an internal plane spacing of 1.9 nm was found (inset of Figure 1A).[30] As shown in Figure 1B, for the Ti_3C_2 samples,[31] the adsorption peak at 1052 cm^{-1} was related to the C−F bond, while the peak at 1272 cm^{-1} was related to the C−O bond. The adsorption peak at 1631 cm^{-1} represented the bending vibration of −OH, while the peak at 3456 cm^{-1} was related to the asymmetric stretching of −OH. In addition, we used XRD to study the crystal structure of Ti_3C_2. We can see from Figure 1C that when the MAX phase reacted with LiF/HCl solution, the strongest diffraction peak of Ti_3AlC_2 (104) disappeared in the XRD spectrum of Ti_3C_2.[32] The XRD pattern of the Ti_3C_2 further confirmed the successful synthesis of the material as the observed diffraction peaks were consistent with the literature values.[33] Moreover, the EDS pattern (Figure 1D) displayed the successful etching of elemental Al and the coexistence of elements Ti and C in the electrode surface. We also used AFM to analyze the morphology and thickness of Ti_3C_2. As shown in Figure S1, obvious lamellar structures were observed. We can see from Figure S1B that the height of Ti_3C_2 nanosheets was about 2.5 nm, in agreement with the reported literature.[34]

3.2. Characterization of HRP/Ti_3C_2/Nafion/GCE Biosensor. Ti_3C_2 has a graphene-like two-dimensional nanosheet structure, which is convenient for HRP to combine with it. Meanwhile, Ti_3C_2 has good electron transfer ability, making it an excellent material for fabricating a H_2O_2 electrochemical biosensor. Studies have shown that Nafion is a good film forming material, which can form a unique film on the surface of the electrode. The electrochemical performance of the biosensor was studied. The CV and DPV responses of GCE, Ti_3C_2/GCE, HRP/Ti_3C_2/Nafion/GCE, and HRP/Nafion/GCE in the 1 mM $K_3[Fe(CN)_6]$ and 0.1 M KCl were shown in Figure 2A,B. The voltammetric peaks of the HRP/

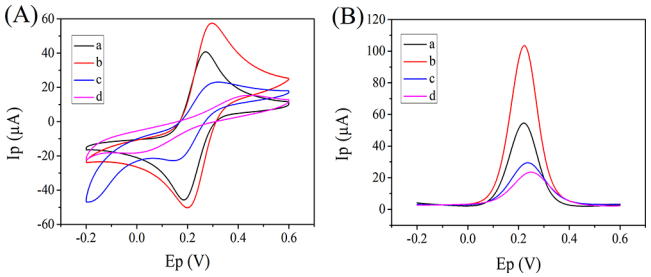

Figure 2. (A) CV and (B) DPV of the biosensor; curves a−d represent bare GCE, Ti_3C_2/GCE, HRP/Ti_3C_2/Nafion/GCE, and HRP/Nafion/GCE, respectively. The experiments were carried out in PBS (pH 7.4) containing 1 mM $K_3[Fe(CN)_6]$ and 0.1 M KCl.

Ti_3C_2/Nafion-modified electrochemical biosensor were derived from the oxidation and reduction reaction of $K_3[Fe(CN)_6]$. The results showed that Ti_3C_2/GCE (curve b) had a higher redox peak than bare GCE (curve a), indicating that Ti_3C_2 could enhance electron transfer. When HRP/Nafion was attached (curves c and d), the peak current decreased, because the biomolecules fixed at the electrode interface hinder the electron transfer.

We could see from Figure 1B that HRP demonstrated characteristic peaks at 2957, 1651, 1532, and 1071 cm^{-1}.[35] The adsorption peak at 1651 cm^{-1} was related to the α-helical conformation of the HRP. Meanwhile, the peak at 1532 cm^{-1} was related to the β-sheet conformation of the HRP. Following immobilization of HRP onto the two-dimensional Ti_3C_2 nanosheets, the major bands of HRP could be observed on the FT-IR spectra of HRP/Ti_3C_2, indicating a successful immobilization process without any conformational change in the secondary structure of HRP.

3.3. Principle of the Analytical Methods. The principle of this experiment was based on the specific effect of HRP on H_2O_2. In this paper, an HRP/Ti_3C_2/Nafion/GCE biosensor was prepared using Ti_3C_2 as the base material, and Nafion as a film forming material with good performance. Ti_3C_2 can accelerate the electron transfer between the active center of the enzyme. Nafion facilitated the dispersion of Ti_3C_2 and helped to form a uniform and stable film on the surface of the electrode. The biosensor can detect H_2O_2 with high sensitivity.

The electrochemical performance of the HRP/Ti_3C_2/Nafion/GCE biosensor was analyzed by DPV. The voltammetric peaks of the HRP/Ti_3C_2/Nafion-modified electrochemical biosensor derived from HRP catalyze H_2O_2 to produce electron transfer. As shown in Figure 3A, the peak current significantly increases in the presence of Ti_3C_2, which proves that Ti_3C_2 has excellent conductive properties. ΔIp represents the current difference measured by the biosensor for H_2O_2 and blank solution, respectively. As shown in Figure 3B, ΔIp changes further proved that Ti_3C_2 has a good electrochemical response and catalytic performance. This is because Ti_3C_2 has a high specific surface area and excellent electrochemical properties, that are conducive to the occurrence of the oxidation reaction.

3.4. Optimization of the Proportion of Film Composition and Reaction Conditions. The performance of the biosensor was optimized by adjusting the dosage of Ti_3C_2, HRP, and Nafion; the pH of the buffer; and the incubation time. In Figure 4A,B, the change of the peak current of the biosensor at different component concentration ratios showed that the peak current reached its maximum value at 1/3/60 of

https://doi.org/10.1021/acsbiomaterials.1c00242
ACS Biomater. Sci. Eng. 2021, 7, 2767−2773

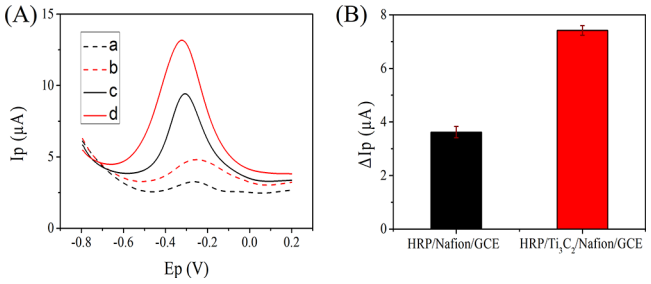

Figure 3. (A) Ip curves a and b represent HRP/Nafion/GCE and HRP/Ti_3C_2/Nafion/GCE in PBS (pH 7.4), respectively. The curves c and d represent HRP/Nafion/GCE and HRP/Ti_3C_2/Nafion/GCE in PBS (pH 7.4) comprising 1 mM H_2O_2, respectively. (B) The ΔIp of the peak current of H_2O_2 catalyzed by HRP/Nafion/GCE and HRP/Ti_3C_2/Nafion/GCE, respectively.

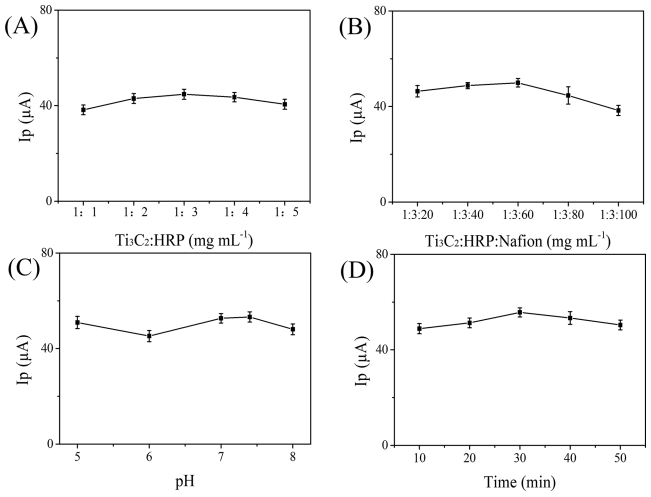

Figure 4. Effects of various conditions on the determination of H_2O_2: (A) mass concentration ratio of Ti_3C_2 and HRP; (B) mass concentration ratio of Ti_3C_2, HRP, and Nafion; (C) the pH value of the sensing system; (D) incubation time.

Ti_3C_2/HRP/Nafion. In addition, as shown in Figure 4C, the peak current of the biosensor increased from pH 6, reached the maximum value at pH 7.4, and decreased at pH 8. Finally, the incubation time also has a great influence on the peak current. We could see from Figure 4D that when the reaction time was 30 min, the peak current was maximized. Therefore, the mass concentration ratio of Ti_3C_2/HRP/Nafion = 1:3:60, PBS (pH 7.4), and an incubation time of 30 min were used to prepare the biosensor and analyze the reaction system.

3.5. Linearity, Selectivity, and Storage Stability of the Biosensor. In order to illustrate the analytical performance of this biosensor, we measured different concentrations of H_2O_2 under optimal conditions. We can see from Figure 5A,B that the current response displayed a linear range of 5−8000 μM, and a detection limit of 1 μM. As shown in Figure 5C, the selectivity of the fabricated HRP/Ti_3C_2/Nafion/GCE biosensor was evaluated using potentially interfering substances including AA, UA, urea, CA, and Glu. The concentration of interfering substance is 10 times that of the target substance. The results show that the biosensor has good selectivity to H_2O_2. The HRP/Ti_3C_2/Nafion/GCE biosensor can maintain about 98% of its original performance at 4 °C for 48 h, but the HRP/Nafion/GCE biosensor drops to about 40% of its original performance (Figure 5D). The results show that the

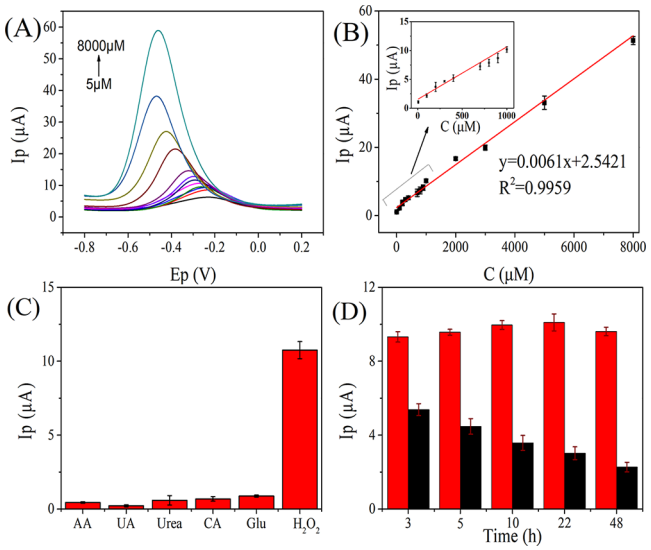

Figure 5. (A) DPV response of the biosensor to the detection of different concentrations of H_2O_2 in PBS (pH 7.4). (B) The corresponding regression graph illustrates the peak oxidation current of different concentrations of H_2O_2. (C) Selectivity of H_2O_2 detection. (D) Stability of the HRP/Ti_3C_2/Nafion/GCE biosensor (red) and stability of the HRP/Nafion/GCE biosensor (black).

HRP/Ti_3C_2/Nafion film has more advantages in stability. In order to verify the precision of the biosensor, different batches of biosensors were used for the determination of H_2O_2 (Figure S2). The RSD was calculated to be 1.6%, indicating that the biosensor we built has high precision.

3.6. Analysis of H_2O_2 in Human Serum. The application of this method was explored by detecting serum H_2O_2 in normal controls and patients with AMI. As shown in Figure 6,

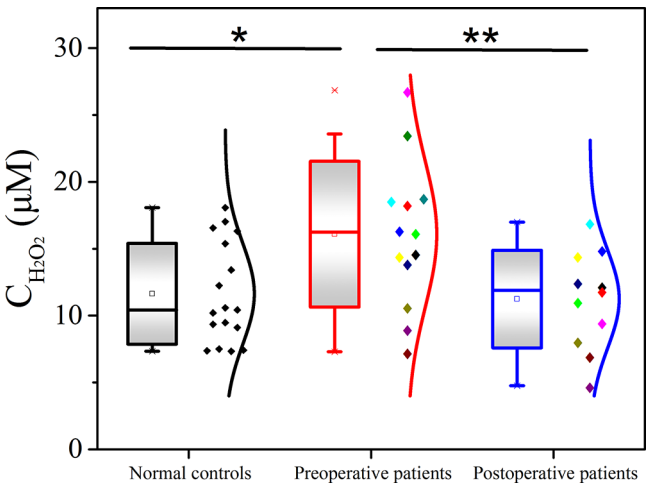

Figure 6. Serum H_2O_2 levels in group of normal controls, preoperative AMI patients, and postoperative AMI patients. *P < 0.05, **P < 0.01. The dots of the same color represent the preoperative and postoperative H_2O_2 levels of the same person.

serum samples from 17 normal controls, 13 preoperative patients, and 11 postoperative patients (2 patients did not perform PCI) were measured. An unpaired t test conducted between normal controls and preoperative patients (P = 0.0131) suggested that the level of H_2O_2 in the serum of preoperative patients was higher than that of normal controls,

https://doi.org/10.1021/acsbiomaterials.1c00242
ACS Biomater. Sci. Eng. 2021, 7, 2767−2773

which was consistent with literature studies that have been reported.[36,37] The reason may be that oxidative stress leads to excess production of H_2O_2.[38] This result indicates that H_2O_2 may be an important indicator of AMI. The paired t test between preoperative and postoperative patients ($P = 0.0040$) showed a dramatic reduction of the serum H_2O_2 level after PCI, suggesting that the reperfusion therapy for PCI improved the stress status as well as a responsive reduction of oxidative substances in the body. These results suggested that H_2O_2 can be used as an index for evaluating the therapeutic effect of coronary intervention in clinical practice.

We could see from Table 1 that the concentration of H_2O_2 in normal controls was 8.16 μM. Three normal control samples were taken and added with 50%, 100%, and 150% H_2O_2 of the previously measured concentrations. The sample recovery rate was 97.80%−98.43%, which verified the accuracy and reliability of the method in actual samples. Moreover, we compared this method with two different commercially available hydrogen peroxide detection kits. As shown in Figure S3, the results of the biosensor were consistent with the results of the hydrogen peroxide detection kits.

Table 1. Recovery Test for Determination of H_2O_2 in Human Serum ($n = 3$)

sample	detected H_2O_2 (μM)	added H_2O_2 (μM)	found H_2O_2 (μM)	recovery (%)
normal control	8.16	4.08	11.98	97.88
		8.16	15.96	97.80
		12.24	20.08	98.43

As shown in Table 2, the fabricated biosensor has an excellent performance compared with those of several typical enzyme-catalyzed H_2O_2 sensors previously reported. This may be because Ti_3C_2 has a large specific surface area and good electrochemical activity. Therefore, the HRP/Ti_3C_2/Nafion/GCE could be used for the detection of H_2O_2 in human serum.

Table 2. Comparison of Several H_2O_2 Biosensors

sensor	linear range (μM)	LOD (μM)	ref
β-CDP/cationic dye/HRP/GCE	1000−1100	500	39
GS Nafion-Fe_3O_4/Au/HRP	20−2500	12	40
clay-HRP-clay/AuCS	39−3100	9	41
HRP/LDH-CMC	20−6000	12.4	14
HRP/MoS_2/GC	1−950	0.26	42
AgNPs-rGO-PANI/GCE	0.01−1000		43
3D Cu_2O-GA	1−1470	0.37	44
HRP/Ti_3C_2/Nafion/GCE	5−8000	1	this work

4. CONCLUSIONS

In summary, we prepared a new electrochemical biosensor based on HRP/Ti_3C_2/Nafion film for the determination of H_2O_2. Combining Ti_3C_2 with enzymes can improve the stability and sensitivity of the biosensor. Moreover, the fabricated biosensor exhibited a wide linear range from 5 to 8000 μM and a detection limit of 1 μM. Because of its high sensitivity and simple operation, this method has a good clinical application prospect. This study is the first to use the electrochemical biosensors based on HRP/Ti_3C_2/Nafion film for the H_2O_2 level analysis of serum samples from patients with AMI before and after the operation. The clinical evaluation of PCI is generally based on the relief of patients' symptoms, but this study may provide a molecular level evaluation method of the therapeutic effect. The important application prospect of this method in the real-time diagnosis of AMI disease and evaluation of the surgical treatment effect is suggested.

■ ASSOCIATED CONTENT

Supporting Information

The Supporting Information is available free of charge at https://pubs.acs.org/doi/10.1021/acsbiomaterials.1c00242.

AFM image of the Ti_3C_2-MXene nanosheets and AFM height profiles, determination values of 1 mM H_2O_2 by different batches of biosensors, and analytical results of H_2O_2 solution by our electrochemical method and two different commercially available kits (PDF)

■ AUTHOR INFORMATION

Corresponding Authors

Wanying Zhu − *School of Pharmacy, Nanjing Medical University, Nanjing, Jiangsu 211166, China*; Email: wanyingzhu@njmu.edu.cn

Xuemin Zhou − *School of Pharmacy, Nanjing Medical University, Nanjing, Jiangsu 211166, China*; orcid.org/0000-0001-7717-0436; Email: xueminzhou001_001@hotmail.com

Authors

Wei Xu − *School of Pharmacy, Nanjing Medical University, Nanjing, Jiangsu 211166, China*

Marwan Sakran − *School of Pharmacy, Nanjing Medical University, Nanjing, Jiangsu 211166, China*

Jianwen Fei − *School of Pharmacy, Nanjing Medical University, Nanjing, Jiangsu 211166, China*

Xiaoyun Li − *School of Pharmacy, Nanjing Medical University, Nanjing, Jiangsu 211166, China*

Chenyuan Weng − *School of Pharmacy, Nanjing Medical University, Nanjing, Jiangsu 211166, China*

Wei Yang − *School of Pharmacy, Nanjing Medical University, Nanjing, Jiangsu 211166, China*

Guomin Zhu − *Nanjing Yimin Hospital, Nanjing, Jiangsu 211100, China*

Complete contact information is available at: https://pubs.acs.org/10.1021/acsbiomaterials.1c00242

Notes

The authors declare no competing financial interest.

■ ACKNOWLEDGMENTS

This work was supported by the National Natural Science Foundation of China (No. 81773681, 81572081, 21904069) and the Natural Science Foundation of Jiangsu Province (No. BK20190653). This work was also supported by Chinese Postdoctoral Science Foundation (No. 2019M661777) and the Postdoctoral Science Foundation of Jiangsu (No. 2019K068, 2019Z176).

■ REFERENCES

(1) Lu, Q.; Wang, J.; Li, B.; Weng, C.; Li, X.; Yang, W.; Yan, X.; Hong, J.; Zhu, W.; Zhou, X. Dual-Emission Reverse Change Ratio Photoluminescence Sensor Based on a Probe of Nitrogen-Doped

Ti_3C_2 Quantum Dots/DAP to Detect H_2O_2 and Xanthine. *Anal. Chem.* **2020**, *92* (11), 7770−7777.
(2) Wang, X.; Jiang, Y.; Zhang, Q.; Tian, X.; Sun, Q.; Guo, D.; Wang, Q.; Chai, X.; Peng, L.; Li, C.; Wang, Y. Autophagy as a novel insight into mechanism of Danqi pill against post-acute myocardial infarction heart failure. *J. Ethnopharmacol.* **2021**, *266*, 113404.
(3) Anderson, J. L.; Morrow, D. A. Acute Myocardial Infarction. *N. Engl. J. Med.* **2017**, *376*, 2053−64.
(4) Huynh, T.; Perron, S.; O'Loughlin, J.; Joseph, L.; Labrecque, M. V.; Tu, J.; Théroux, P. Comparison of Primary Percutaneous Coronary Intervention and Fibrinolytic Therapy in ST-Segment-Elevation Myocardial Infarction: Bayesian Hierarchical Meta-Analyses of Randomized Controlled Trials and Observational Studies. *Circulation* **2009**, *119*, 3101−3109.
(5) Mehta, S.; Cannon, C.; Fox, K.; Wallentin, L.; Boden, W.; Spacek, R.; Widimsky, P.; McCullough, P.; Hunt, D.; Braunwald, E.; Yusuf, S. Routine vs Selective Invasive Strategies in Patients With Acute Coronary Syndromes. *American Medical Association* **2005**, *293* (23), 2908.
(6) Bagatini, M.; Martins, C.; Battisti, V.; Gasparetto, D.; da Rosa, C. S.; Spanevello, R.; Ahmed, M.; Schmatz, R.; Schetinger, M.; Morsch, V. Oxidative stress versus antioxidant defenses in patients with acute myocardial infarction. *Heart Vessels* **2011**, *26* (1), 55−63.
(7) Ekeløf, S.; Jensen, S.; Rosenberg, J.; Gögenur, I. Reduced Oxidative Stress in STEMI Patients Treated by Primary Percutaneous Coronary Intervention and with Antioxidant Therapy: A Systematic Review. *Cardiovasc. Drugs Ther.* **2014**, *28* (2), 173−181.
(8) Pandey, N.; Kaur, G.; Chandra, M.; Sanwal, G.; Misra, M. Enzymatic oxidant and antioxidants of human blood platelets in unstable angina and myocardial infarction. *Int. J. Cardiol.* **2000**, *76* (1), 33−38.
(9) Fu, L.; Wang, A.; Xie, K.; Zhu, J.; Chen, F.; Wang, H.; Zhang, H.; Su, W.; Wang, Z.; Zhou, C.; Ruan, S. Electrochemical detection of silver ions by using sulfur quantum dots modified gold electrode. *Sens. Actuators, B* **2020**, *304*, 127390.
(10) Zhang, R.; Chen, W. Recent advances in graphene-based nanomaterials for fabricating electrochemical hydrogen peroxide sensors. *Biosens. Bioelectron.* **2017**, *89*, 249−268.
(11) Yu, Z.; Cai, G.; Liu, X.; Tang, D. Platinum Nanozyme-Triggered Pressure-Based Immunoassay Using a Three-Dimensional Polypyrrole Foam-Based Flexible Pressure Sensor. *ACS Appl. Mater. Interfaces* **2020**, *12* (36), 40133−40140.
(12) Zhang, B.; Tang, D.; Goryacheva, I. Y.; Niessner, R.; Knopp, D. Anodic-Stripping Voltammetric Immunoassay for Ultrasensitive Detection of Low-Abundance Proteins Using Quantum Dot Aggregated Hollow Microspheres. *Chem. - Eur. J.* **2013**, *19* (7), 2496−2503.
(13) Zeng, R.; Luo, Z.; Zhang, L.; Tang, D. Platinum Nanozyme-Catalyzed Gas Generation for Pressure-Based Bioassay Using Polyaniline Nanowires-Functionalized Graphene Oxide Framework. *Anal. Chem.* **2018**, *90* (20), 12299−12306.
(14) Yuan, J.; Xu, S.; Zeng, H.; Cao, X.; Dan Pan, A.; Xiao, G.; Ding, P. Hydrogen peroxide biosensor based on chitosan/2D layered double hydroxide composite for the determination of H_2O_2. *Bioelectrochemistry* **2018**, *123*, 94−102.
(15) Wu, L.; Lu, X.; Dhanjai; Wu, Z.-S.; Dong, Y.; Wang, X.; Zheng, S.; Chen, J. 2D transition metal carbide MXene as a robust biosensing platform for enzyme immobilization and ultrasensitive detection of phenol. *Biosens. Bioelectron.* **2018**, *107*, 69−75.
(16) Wu, L.; Deng, D.; Jin, J.; Lu, X.; Chen, J. Nanographene-based tyrosinase biosensor for rapid detection of bisphenol A. *Biosens. Bioelectron.* **2012**, *35* (1), 193−199.
(17) Zhang, H.; Wang, Z.; Zhang, Q.; Wang, F.; Liu, Y. Ti_3C_2 MXenes nanosheets catalyzed highly efficient electrogenerated chemiluminescence biosensor for the detection of exosomes. *Biosens. Bioelectron.* **2019**, *124−125*, 184−190.
(18) Cardoso, R. M.; Silva, P. R.L.; Lima, A. P.; Rocha, D. P.; Oliveira, T. C.; do Prado, T. M.; Fava, E. L.; Fatibello-Filho, O.; Richter, E. M.; Munoz, R. A.A. 3D-Printed graphene/polylactic acid electrode for bioanalysis: Biosensing of glucose and simultaneous determination of uric acid and nitrite in biological fluids. *Sens. Actuators, B* **2020**, *307*, 127621.
(19) Xu, R.; Chi, C.; Li, F.; Zhang, B. Immobilization of horseradish peroxidase on electrospun microfibrous membranes for biodegradation and adsorption of bisphenol A. *Bioresour. Technol.* **2013**, *149*, 111−116.
(20) Bilal, M. M.N.; Iqbal, H.; Hu, H.; Wang, W.; Zhang, X. Development of horseradish peroxidase-based cross-linked enzyme aggregates and their environmental exploitation for bioremediation purposes. *J. Environ. Manage.* **2017**, *188*, 137−143.
(21) Naguib, M.; Kurtoglu, M.; Presser, V.; Lu, J.; Niu, J.; Heon, M.; Hultman, L.; Gogotsi, Y. W.; Barsoum, M. Two-Dimensional Nanocrystals Produced by Exfoliation of Ti_3AlC_2. *Adv. Mater.* **2011**, *23* (37), 4248−4253.
(22) Naguib, M. N.; Mochalin, V. W.; Barsoum, M.; Gogotsi, Y. 25th Anniversary Article: MXenes: A New Family of Two-Dimensional Materials. *Adv. Mater.* **2014**, *26* (7), 992−1005.
(23) Ghidiu, M. R.; Lukatskaya, M.; Zhao, M.; Gogotsi, Y. W.; Barsoum, M. Conductive two-dimensional titanium carbide'clay'with high volumetric capacitance. *Nature* **2014**, *516* (7529), 78−81.
(24) Chen, J.; Tong, P.; Huang, L.; Yu, Z.; Tang, D. Ti_3C_2 MXene nanosheet-based capacitance immunoassay with tyramine-enzyme repeats to detect prostate-specific antigen on interdigitated microcomb electrode. *Electrochim. Acta* **2019**, *319*, 375−381.
(25) Cai, G.; Yu, Z.; Tong, P.; Tang, D. Ti_3C_2 MXene quantum dot-encapsulated liposomes for photothermal immunoassays using a portable near-infrared imaging camera on a smartphone. *Nanoscale* **2019**, *11* (33), 15659−15667.
(26) Mohammadniaei, M.; Koyappayil, A.; Sun, Y.; Min, J.; Lee, M. Gold nanoparticle/MXene for multiple and sensitive detection of oncomiRs based on synergetic signal amplification. *Biosens. Bioelectron.* **2020**, *159*, 112208.
(27) Yu, Z.; Lv, S.; Ren, R.; Cai, G.; Tang, D. Photoelectrochemical sensing of hydrogen peroxide at zero working potential using a fluorine-doped tin oxide electrode modified with $BiVO_4$ microrods. *Microchim. Acta* **2017**, *184* (3), 799−806.
(28) Lin, Y.; Chen, X.; Lin, Y.; Zhou, Q.; Tang, D. Non-enzymatic sensing of hydrogen peroxide using a glassy carbon electrode modified with a nanocomposite made from carbon nanotubes and molybdenum disulfide. *Microchim. Acta* **2015**, *182* (9−10), 1803−1809.
(29) Chen, Y.; Xie, X.; Xin, X.; Tang, Z.; Xu, Y. $Ti_3C_2T_x$-Based Three-Dimensional Hydrogel by a Graphene Oxide-Assisted Self-Convergence Process for Enhanced Photoredox Catalysis. *ACS Nano* **2019**, *13* (1), 295−304.
(30) Zuo, D.; Song, S.; An, C.; Tang, L.; He, Z.; Zheng, J. Synthesis of sandwich-like structured Sn/SnOx/MXene composite through in-situ growth for highly reversible lithium storage. *Nano Energy* **2019**, *62*, 401−409.
(31) Xiu, L.; Wang, Z.; Yu, M.; Wu, X.; Qiu, J. Aggregation-Resistant 3D MXene-Based Architecture as Efficient Bifunctional Electrocatalyst for Overall Water Splitting. *ACS Nano* **2018**, *12* (8), 8017−8028.
(32) Ding, M.; Chen, W.; Xu, H.; Shen, Z.; Lin, T.; Hu, K.; Lu, C.; Xie, Z. Novelα-Fe_2O_3/MXene nanocomposite as heterogeneous activator of peroxymonosulfate for the degradation of salicylic acid. *J. Hazard. Mater.* **2020**, *382*, 121064.
(33) Lukatskaya, M.; Mashtalir, O.; Ren, C.; Dall'Agnese, Y.; Rozier, P.; Taberna, P.; Naguib, M.; Simon, P.; Barsoum, M.; Gogotsi, Y. Cation Intercalation and High Volumetric Capacitance of Two-Dimensional Titanium Carbide. *Science* **2013**, *341* (6153), 1502−1505.
(34) Lipatov, A.; Alhabeb, M.; Lukatskaya, M.; Boson, A.; Gogotsi, Y.; Sinitskii, A. Effect of Synthesis on Quality, Electronic Properties and Environmental Stability of Individual Monolayer Ti_3C_2 MXene Flakes. *Advanced Electronic Materials* **2016**, *2* (12), 1600255.
(35) Dai, H.; Lü, W.; Zuo, X.; Zhu, Q.; Pan, C.; Niu, X.; Liu, J.; Chen, H.; Chen, X. A novel biosensor based on boronic acid functionalized metal-organic frameworks for the determination of

https://doi.org/10.1021/acsbiomaterials.1c00242
ACS Biomater. Sci. Eng. 2021, 7, 2767−2773

hydrogen peroxide released from living cells. *Biosens. Bioelectron.* **2017**, *95*, 131−137.
(36) Yao, W.; Cao, Y.; She, M.; Yan, Y.; Li, J.; Leng, X.; Liu, P.; Zhang, S.; Li, J. Imaging and Monitoring the Hydrogen Peroxide Level in Heart Failure by a Fluorescent Probe with a Large Stokes Shift. *ACS Sensors* **2021**, *6* (1), 54−62.
(37) Schenkel, P.; Tavares, A.; Fernandes, R.; Diniz, G.; Ludke, A.; Ribeiro, M.; da Rosa Araujo, A. S.; Barreto-Chaves, M.; Bello-Klein, A. Time course of hydrogen peroxide-thioredoxin balance and its influence on the intracellular signalling in myocardial infarction. *Experimental Physiology* **2012**, *97* (6), 741−749.
(38) Almzaiel, A. Oxidative stress and inflammation in ischemic heart disease: role of trace elements, oxidants and antioxidants. *Journal of Contemporary Medical Sciences* **2015**, *1* (2), 18−22.
(39) Zhu, M.; Han, S.; Yuan, Z. *β*-Cyclodextrin polymer as the immobilization matrix for peroxidase and mediator in the fabrication of a sensor for hydrogen peroxide. *J. Electroanal. Chem.* **2000**, *480*, 255−261.
(40) Xin, Y.; Fu-bing, X.; Hong-wei, L.; Feng, W.; Di-zhao, C.; Zhao-yang, W. A novel H_2O_2 biosensor based on Fe_3O_4-Au magnetic nanoparticles coated horseradish peroxidase and graphene sheets-Nafion film modified screen-printed carbon electrode. *Electrochim. Acta* **2013**, *109*, 750−755.
(41) Zhao, X.; Mai, Z.; Kang, X.; Zou, X. Direct electrochemistry and electrocatalysis of horseradish peroxidase based on clay-chitosan-gold nanoparticle nanocomposite. *Biosens. Bioelectron.* **2008**, *23* (7), 1032−1038.
(42) Wang, G.; Bao, W.; Wang, J.; Lu, Q.; Xia, X. Immobilization and catalytic activity of horseradish peroxidase on molybdenum disulfide nanosheets modified electrode. *Electrochem. Commun.* **2013**, *35*, 146−148.
(43) Kumar, V.; Gupta, R.; Gundampati, R.; Singh, D.; Mohan, S.; Hasan, S.; Malviya, M. Enhanced electron transfer mediated detection of hydrogen peroxide using a silver nanoparticle-reduced graphene oxide-polyaniline fabricated electrochemical sensor. *RSC Adv.* **2018**, *8* (2), 619−631.
(44) Cheng, C.; Zhang, C.; Gao, X.; Zhuang, Z.; Du, C.; Chen, W. 3D Network and 2D Paper of Reduced Graphene Oxide/Cu_2O Composite for Electrochemical Sensing of Hydrogen Peroxide. *Anal. Chem.* **2018**, *90* (3), 1983−1991.

https://doi.org/10.1021/acsbiomaterials.1c00242
ACS Biomater. Sci. Eng. 2021, 7, 2767−2773